

Estimation of Correlation Matrices from Limited time series Data using Machine Learning

Nikhil Easaw^a, Woo Soek^{b,c}, Prashant Singh Lohiya^a, Sarika Jalan^a, Priodyuti Pradhan^d

^a *Complex Systems Lab, Department of Physics, Indian Institute of Technology Indore, Khandwa Road, Simrol, Indore-453552, India*

^b *Center for Theoretical Physics of Complex Systems, Institute for Basic Science (IBS), Daejeon 34126, Republic of Korea*

^c *1ST Biotherapeutics, Inc., Seongnam, 13493, Republic of Korea*

^d *School of Computer Science, University of Petroleum and Energy Studies, Dehradun - 248007, India*

Abstract

Prediction of correlation matrices from given time series data has several applications for a range of problems, such as inferring neuronal connections from spiking data, deducing causal dependencies between genes from expression data, and discovering long spatial range influences in climate variations. Traditional methods of predicting correlation matrices utilize time series data of all the nodes of the underlying networks. Here, we use a supervised machine learning technique to predict the correlation matrix of entire systems from finite time series information of a few randomly selected nodes. The accuracy of the prediction from the model confirms that only a limited time series of a subset of the entire system is enough to make good correlation matrix predictions. Furthermore, using an unsupervised learning algorithm, we provide insights into the success of the predictions from our model. Finally, we apply the machine learning model developed here to real-world data sets.

Keywords: Time series data, Correlation matrix, Non-linear dynamics, Machine learning, Complex networks

1. Introduction

Machine learning has been applied in diverse areas of physical sciences ranging from condensed matter to high energy physics to complex systems. In complex systems, neural network-based machine learning techniques have been used in predicting amplitude death [1], anticipation of synchronization [2], phase transitions in complex networks [3], time series prediction [4], etc. In particular, forecasting time series data has attracted interest from the scientific fraternity due to its diverse applications in real-world dynamical systems like stock markets and the brain. However, predicting the time series of a dynamical system has many limitations [5, 6]. Since every data point in a time series is a function of the previous time steps, the error in predicting the future time series data points compounds over time. To avoid prediction error, the correlation matrix of the time series is preferred over the direct prediction of the future time series data points. A correlation matrix of a given multivariate time series data set is useful in several practical real-world scenarios

Email addresses: sarika@iiti.ac.in (Sarika Jalan), priodyutipradhan@gmail.com (Priodyuti Pradhan)

[7, 8]. For instance, by considering fMRI or MEG signals from several brain regions as time series data, one can construct the corresponding correlation matrix, which can then be used to extract the adjacency matrix by setting a threshold value [9, 10, 11].

In most cases, one calculates average correlation matrices of a given time series data. A correlation matrix of time series data may vary depending on the length of observations and temporal position. Two well-known methods of estimating a true correlation matrix are; (i) the maximum likelihood estimation (MLE) and (ii) the graphical least absolute shrinkage and selection operator method (GLASSO). The MLE method first assumes a sample correlation matrix from a Gaussian distribution that is iteratively corrected to estimate an actual correlation matrix by maximizing the likelihood of observing the given time series data. The GLASSO method [12] is an extension of the MLE method for those cases where MLE can not be applied, for example, if the dimensionality of the Gaussian distribution is higher than the available number of observation samples. Furthermore, a prerequisite of these techniques is to have information on time series data of all the network nodes, whereas, in real-world systems, often time series information of limited nodes are available. Therefore, these methods stall modelling cases where the number of time series is much lesser than the number of nodes forming the corresponding system.

Here we develop a machine learning framework to reconstruct a full correlation matrix from time series data of a few nodes. By considering two different dynamical systems, we demonstrate that the supervised learning method can predict the correlation matrix from the limited time series data of a few nodes. Furthermore, by analyzing the mean square error (MSE) between the true and the predicted correlation matrices, we confirm that only a limited time series data for a subset of nodes is enough for accomplishing good predictions. The correlation matrices are predicted using either by considering higher degree nodes or by considering lower degree nodes of a given network. The prediction accuracy for both cases is observed to be the same, indicating that the degree of the available nodes does not impact the prediction of a correlation matrix. Furthermore, we use an unsupervised learning algorithm (UMAP) to provide insights into our forecasts. Finally, we use real-world EEG data sets to validate our model.

The article is organized as follows: Section 2 discusses the graphs, dynamical, and machine learning models. It also contains the notations and definitions used in the paper. Section 3 illustrates the time series data generation, results, and analysis. Finally, section 4 summarizes our study.

2. Preliminary

Consider an un-directed graph or network, $\mathcal{G} = \{V, E\}$ where $V = \{v_1, \dots, v_n\}$ is the set of vertices (nodes) and $E = \{(v_i, v_j) | v_i, v_j \in V\}$ is the set of edges (connections) which contains the unordered pairs of vertices. We denote the adjacency matrix corresponding to \mathcal{G} as $\mathbf{A} \in \mathbb{R}^{n \times n}$ which is defined as $A_{ij} = 1$ if nodes i and j are connected, and 0 otherwise. The $|V| = N$ and $|E| = M$ represent the number of nodes and number of edges in \mathcal{G} , respectively. The number of edges linked to a particular node v_i is referred to as its degree and denoted by $k_i = \sum_{j=1}^n a_{ij}$. The average degree of the network is denoted by $\langle k \rangle = \frac{1}{n} \sum_{i=1}^n k_i$. We use two random graph models, the Erdős-Rényi (ER) and the Scale-Free (SF) networks, to model the coupled dynamical systems [13]. The ER random model network or the graph-valued random variable with the parameters is denoted by $\mathcal{G}^{ER}(N, p)$ where N is the number of nodes and p is the edge probability [14]. The existence of each edge is statistically independent of all other edges. When we refer to ‘the graph

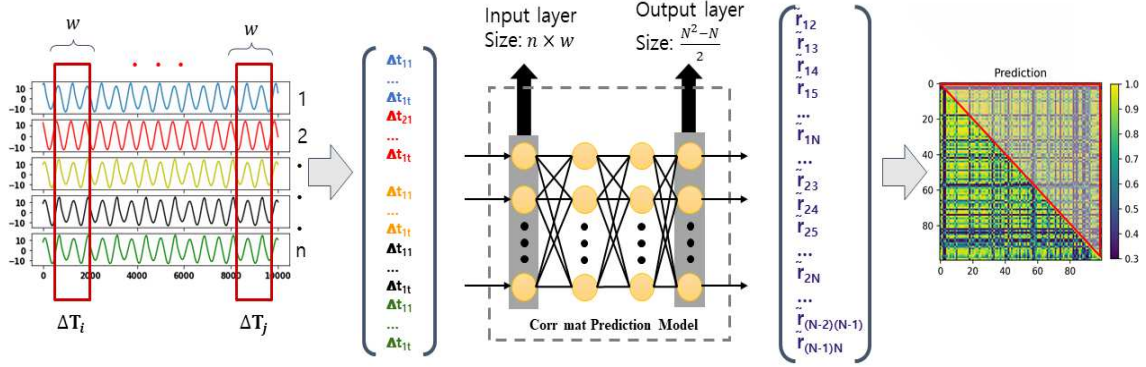


Figure 1: Schematic representation of ML model structure. Input to the model is partial time series from a few nodes ($n < N$) in the shape of a time series window ($\Delta T_q \in \mathbb{R}^{n \times w}$). Time windows are flattened to a column vector ($n \times w$) and fed into the input layer. The entire correlation matrix is constructed from the output column vector ($\frac{N^2 - N}{2}$) of the model using the symmetry of the upper triangular part of a correlation matrix.

$\mathcal{G}^{ER}(N, p)$, we mean one *realization* of the random variable with mean degree $\langle k \rangle$ and generated as follows. Starting with N number of nodes, connecting them with a probability $p = N / \langle k \rangle$. The ER random network realization thus generated will have a Binomial degree distribution. The SF networks (\mathcal{G}^{SF}) generated using the Barabási-Albert model follows a power-law degree distribution [13].

2.1. Dynamical Models

We consider chaotic Rössler and FitzHugh-Nagumo neuronal oscillators to model the dynamical evolution of nodes. The coupled dynamics of the nodes on a given graph generate time series data for the entire system. Dynamical evolution of the phase of each node in the network modelled by the Rössler oscillator [15] can be given by:

$$\begin{aligned}
 \dot{x}_i &= -\omega_i y_i - z_i + \lambda_R \sum_{j=1}^N A_{ij} (x_j - x_i) \\
 \dot{y}_i &= \omega_i x_i + 0.15 y_i \\
 \dot{z}_i &= 0.2 + z_i (x_i - 10)
 \end{aligned} \tag{1}$$

where x_i, y_i, z_i for $i = 1, \dots, N$ are the dynamical state variables and ω_i is the natural frequency of i^{th} node which is drawn from a normal distribution with mean 1 and variance 0.03. Here, A_{ij} represents a connection between nodes i and j of \mathcal{G} , and λ_R denotes the overall coupling strength between the connected nodes.

Next, we consider the FitzHugh-Nagumo (FHN) model, which is derived from the works of Hodgkin-Huxley and is famous for its affluence in neuronal dynamics [16]. Many variations of the original FitzHugh-Nagumo model have been developed since it was first introduced. In the present

study, we consider the FHN model given by the following equations [17]:

$$\begin{aligned} \dot{v}_i &= \frac{1}{\delta} [v_i(v_i - a)(1 - v_i) - w_i] + \lambda_F \sum_{j=1}^N A_{ij}(v_j - v_i) \\ \dot{w}_i &= v_i - w_i - b + S(t) \end{aligned} \quad (2)$$

where v_i indicates the membrane potential and w_i stands for the recovery variable of the i^{th} node. Frequency (ω_i) of the driving signal, $S(t) = r \sin \omega_i t$, is drawn from a normal distribution having mean 15 and variance 0.001. Here, λ_F denotes the overall coupling strength. We choose other parameters values of the oscillators as $a = 0.42$, $b = 0.15$, $\delta = 0.005$, and $r = 0.2$. The important parameter for our purpose is the coupling strengths (λ_R and λ_F) and the network realizations encoded in \mathbf{A} . We vary λ_R , λ_F , and \mathbf{A} to generate time series data having different correlation matrices.

2.2. Machine Learning Algorithms

We use a supervised learning algorithm to predict the correlation matrices and an unsupervised learning algorithm to analyze the results. The machine learning model used to predict the correlation matrix is the feed-forward neural network referred to as multi-layer perceptron [18]. The architecture of this model contains one input layer, two hidden layers, and one output layer (Fig. 1). A layer comprises several neurons, and neurons in the adjacent layers are connected. We adopt the SELU (scaled exponential linear unit) as a basic activation function except for the output layer [19]. We use sigmoid as the output activation function when the desired output lies between 0 and 1, and tanh when it is between -1 and 1 . The relationship between the input ($a_j^{(\ell-1)}$) and the output ($a_i^{(\ell)}$) of a layer can be given by,

$$z_i^{(\ell)} = \sum_{j=1}^K w_{ji}^{(\ell-1)} a_j^{(\ell-1)}, \quad a_i^{(\ell)} = \text{SELU}(z_i^{(\ell)}) \quad (3)$$

where w_{ij} is a weighted connection between the j^{th} neuron of the $(\ell - 1)^{th}$ layer and i^{th} neuron of the $(\ell)^{th}$ layer, with K denoting the number of neurons in $(\ell - 1)^{th}$ layer. Value of $a_j^{(\ell)}$ indicates output of j^{th} neuron in the ℓ^{th} layer. The neural network receives an input ($a^{(0)}$) and generates an output ($a^{(L)}$) through the above propagation rule. In our case, $a^{(0)}$ is the input time series window ($\Delta \mathbf{T}_q$), and $a^{(L)}$ is the upper triangular part of the predicted correlation matrix (Fig. 1). Training a neural network means finding a w_{ij} which can give us the desired output (upper triangular part of \mathbf{R}) for a given input window ($\Delta \mathbf{T}_q$) by reducing the difference between the neural network output $a^{(L)}$ and the desired output $\mathbf{Y} \in \mathbb{R}^{N_L}$ (or upper triangular part of \mathbf{R}), where $N_L = \frac{N^2 - N}{2}$. We define this difference in the following manner and call it a loss function, \mathcal{L} .

$$\mathcal{L} = \frac{1}{N_L} \sum_{k=1}^{N_L} (Y_k - a_k^{(L)})^2 \quad (4)$$

We use Adam (Adaptive Moment Estimation) algorithm to minimize the loss function [20]. Furthermore, we use an unsupervised ML approach (UMAP) to gain more insights into the predicted correlation matrices. The UMAP (Uniform Manifold Approximation and Projection) is a manifold

learning technique for dimension reduction [21]. The method preserves the similarity between the vectors in the higher dimension and performs a nonlinear projection to the 2 dimensional space. The UMAP preserves the local and global structures of the data set. Data having similar structures or features are clustered together in low dimensions. The use of UMAP here is two-fold – (a) provides a visual understanding of the predicted correlation matrices with the true correlation matrices, and (b) helps us to select the appropriate training data set to get a meaningful prediction (SI sec. 4).

3. Methods and Results

We predict correlation matrices for cases that closely match real-world scenarios. A dynamic system with a fixed number of nodes can undergo two types of changes (1) coupling strength between nodes can either increase or decrease. (2) a small structural change with rearrangement of links between nodes. We prepare time series data set to match these cases.

3.1. Time series data generation and representation

To prepare data sets, we use two different dynamical models (Rössler and Fitzhugh-Nagumo oscillators) with l different coupling strengths $(\lambda_1, \lambda_2, \dots, \lambda_l)$ on two different model networks (ER and SF) each of having p different realizations $(\mathcal{G}_1, \mathcal{G}_2, \dots, \mathcal{G}_p)$. Hence, we have $d = lp$ different times-series data sets $(\{\mathbf{T}^1, \mathbf{T}^2, \dots, \mathbf{T}^d\})$ as well as true correlation matrices $(\{\mathbf{R}^1, \mathbf{R}^2, \dots, \mathbf{R}^d\})$ for each of the network and dynamical models, respectively. To generate time series data sets, we numerically solve the coupled dynamical systems by varying coupling strength and the realization of model networks. Although on each node of the network, there are three dynamical state variables $(x_i, y_i, \text{ and } z_i)$ for the Rössler (Eq. 1) and two dynamical state variables $(v_i \text{ and } w_i)$ for the FitzHugh-Nagumo oscillators (Eq. 2), we consider only the time evolution of x_i and v_i variables of the oscillators for the time series data sets. After removing the transient part of the time evolution of state variables, we consider time series data sets and construct the corresponding true correlation matrices. For a N size network, we will have N variable time series data, each having length L . The time evolution of N nodes can be represented as a time series matrix $\mathbf{T}^k \in \mathbb{R}^{N \times L}$, $1 \leq k \leq d$ where each row of the matrix represents individual nodes and time evolution of each node is recorded in columns as

$$\mathbf{T}^k = \begin{pmatrix} t_{11}^k & t_{12}^k \dots & t_{1L}^k \\ t_{21}^k & t_{22}^k \dots & t_{2L}^k \\ \vdots & \ddots & \vdots \\ t_{N1}^k & t_{N2}^k \dots & t_{NL}^k \end{pmatrix}, \mathbf{R}^k = \begin{pmatrix} r_{11}^k & r_{12}^k \dots & r_{1N}^k \\ r_{21}^k & r_{22}^k \dots & r_{2N}^k \\ \vdots & \ddots & \vdots \\ r_{N1}^k & r_{N2}^k \dots & r_{NN}^k \end{pmatrix}$$

where t_{ij}^k represents the time series information of the i^{th} node at the j^{th} time step for k^{th} time series data set. The influence of one node on another in a complex system can be represented as the correlation between their time series. We measure the correlation between a pair of time series data of nodes using Pearson correlation coefficient and stored in a matrix $(\mathbf{R}^k \in \mathbb{R}^{N \times N})$ referred to as *true* correlation matrix, where r_{ij}^k represents the correlation between the time series of i^{th} and j^{th} nodes corresponds to k^{th} data set [22].

Since our goal is to predict an entire correlation matrix from the partial information, we roll a window of size $n \times w$ on $\mathbf{T}^k \in \mathbb{R}^{N \times L}$ and creates time series windows $(\Delta \mathbf{T}_q^k \in \mathbb{R}^{n \times w})$ such that $n < N$, $w < L$, $1 \leq q \leq f$, where $f = \lceil ((L - w)/skip) \rceil + 1$ is the number of windows, and skip is

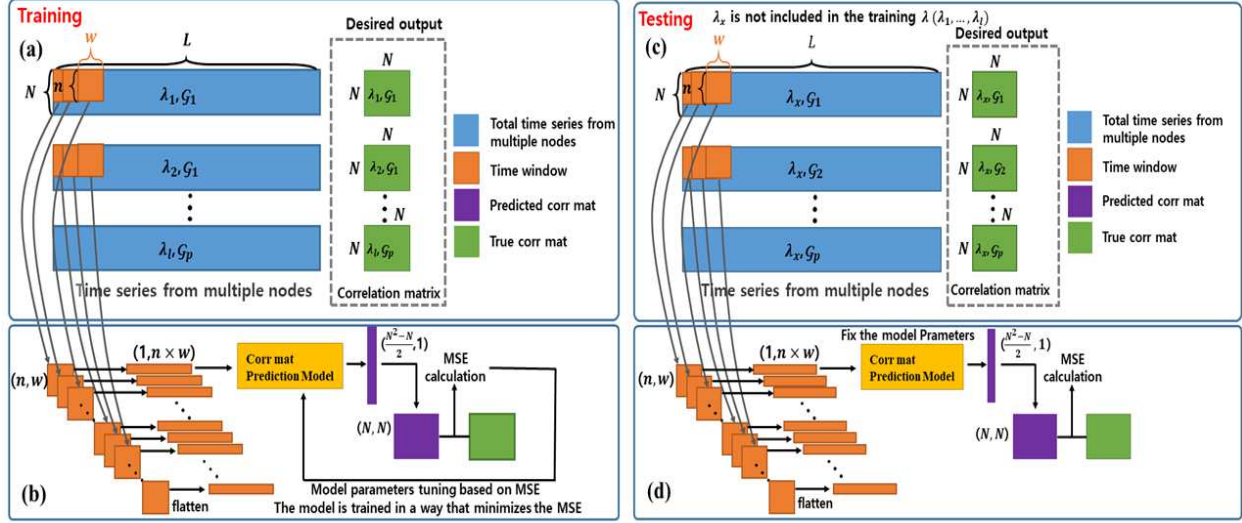


Figure 2: Illustrate the training and testing phase of the machine learning model. For each λ_i , \mathcal{G}_j ($1 \leq i \leq l$, $1 \leq j \leq p$), we have corresponding time series data set and true correlation matrix ($\mathbf{T}^k \in \mathbb{R}^{N \times L}$, $\mathbf{R}^k \in \mathbb{R}^{N \times N}$, $1 \leq k \leq lp$). (a) To use the ML model, we generate time windows of size $n \times w$ ($n < N, w < L$) from the time series data set \mathbf{T}^k and assign the corresponding true correlation matrix as the desired output. (b) The time windows and correlation matrices are flattened to train the ML model. For the correlation matrix, only the upper triangular part is considered. The correlation matrix predicted from a specific time window is used for updating the model parameters by calculating the MSE between the model output (predicted correlation matrix) and desired output (true correlation matrix). (c, d) During the test phase, for a given window as input, the ML model can predict the upper triangular part of the correlation matrix ($\frac{N^2}{2} - N, 1$) as output. The model performance is evaluated by generating time windows from time series not used for training and predicting correlation matrices. All parameters are updated during the training phase and are fixed during the test phase.

the gap between two consecutive windows in time series data (Fig. 2 (a) and (c)). We use these fd windows as inputs to the ML model, that is, training and testing data set (Fig. 2 (b) and (d)). Hence, if we vary n and w , we can create different training and testing data sets. Importantly, during test phase, the ML model predicts a $N \times N$ correlation matrix ($\tilde{\mathbf{R}}_q^k$) from a given $n \times w$ window ($\Delta \mathbf{T}_q^k$). The time series window matrix $\Delta \mathbf{T}_q^k$ and the predicted correlation matrix can be represented as

$$\Delta \mathbf{T}_q^k = \begin{pmatrix} \Delta t_{11} & \Delta t_{12} \dots & \Delta t_{1w} \\ \Delta t_{21} & \Delta t_{22} \dots & \Delta t_{2w} \\ \vdots & \ddots & \vdots \\ \Delta t_{n1} & \Delta t_{n2} \dots & \Delta t_{nw} \end{pmatrix}, \tilde{\mathbf{R}}_q^k = \begin{pmatrix} \tilde{r}_{11} & \tilde{r}_{12} \dots & \tilde{r}_{1N} \\ \tilde{r}_{21} & \tilde{r}_{22} \dots & \tilde{r}_{2N} \\ \vdots & \ddots & \vdots \\ \tilde{r}_{N1} & \tilde{r}_{N2} \dots & \tilde{r}_{NN} \end{pmatrix}$$

with elements Δt_{ab} where $1 \leq a \leq n$, and $1 \leq b \leq w$. To make the notation simpler, we drop q and k from $\Delta t_{q,ab}^k$ and $\tilde{r}_{q,ab}^k$. For our experiment we consider $L = 5000$, $skip = 40$ or 100 and $w \in \{10, 40, 100, 500\}$.

Note that coupling strengths chosen to create time series data sets lie in the semi-synchronous region, i.e., a time series chosen is neither too much correlated nor uncorrelated [23]. If the coupling strength used is such that the time series are too correlated, then the prediction becomes trivial, and if the time series are uncorrelated, then the predictions are of no value. Also, we choose

Models	Rössler (λ_R)	FitzHugh-Nagumo (λ_F)
$\mathcal{G}_1^{ER}, \mathcal{G}_2^{ER}, \dots, \mathcal{G}_{75}^{ER}$	0.012, 0.013, 0.014, 0.015, 0.016	0.28, 0.3, 0.32, 0.34
$\mathcal{G}_1^{SF}, \mathcal{G}_2^{SF}, \dots, \mathcal{G}_{75}^{SF}$	0.005, 0.006, 0.007, 0.008, 0.009	0.24, 0.26, 0.28, 0.3

Table 1: Different network realizations and chosen coupling strength values for time series data generation.

the λ_R and λ_F values from the semi-synchronous region such that correlation values for the time series data to be constant (Fig. S2). More details of choosing the coupling strength values (λ_R and λ_F) are illustrated in SI sec 1. Further note that a linear correlation coefficient is used in measuring the correlation of the time series of the nodes, which is nonlinear. Since there are many different correlation measures, choosing an appropriate measure is essential. The previous research found the Pearson correlation coefficient to be the most relevant and the correlation that provides the system’s most information [24]. However, we also use nonlinear correlation measures (e.g., Spearman correlation [25]) for the real-world data sets, and the prediction results are the same.

3.2. Prediction of correlation matrix for varying coupling strengths and network realizations

For our experiment, we choose $p = 75$ different realizations of the ER random networks and $l = 5$ different coupling strength for Rössler oscillators (Table 1). Hence, we have 375 (training set: 300 and test set: 75) different time series data sets and corresponding true correlation matrices for the Rössler oscillators on ER network realizations. We also choose 4 different coupling strength for the Fitzhugh-Nagumo oscillators on 75 ER network realizations leading to another 300 (training set: 225 and test set: 75) time series data sets. Similarly, we choose 75 different realizations of the SF random networks and 5 different coupling strength for the Rössler oscillators and 4 different coupling strength for the Fitzhugh-Nagumo oscillators. Thus, we have another two different time series data sets on SF network realizations. Finally, we create time series windows for each of the data sets. For example, from 300 training data sets we generate $300 * 124 = 37200$ windows ($f = \lceil ((5000 - 100)/40) \rceil + 1 = 124$) and from 75 test data sets we generate 9300 windows.

In the training phase of the supervised ML algorithm, the input to the model is the set of time series windows and the upper triangular part of the true correlation matrices created from the training data sets (Fig. 2(a, b)). The input time window matrix ($\Delta \mathbf{T}_q^k \in \mathbb{R}^{n \times w}$) and the true correlation matrix ($\mathbf{R}^k \in \mathbb{R}^{N \times N}$) of the whole system are prepared in the shape of a column vector with information of each node, stacked on top of each other to form the vector (Fig. 2(b)). Thus, we assign nw neurons for the input layer and $\frac{N^2 - N}{2}$ for the output layer. Using the loss function (Eq. 4), ML model will update the w_{ij} values (Eq. 3) which will minimize the \mathcal{L} .

During the testing phase, the ML model will only take a time series window and can predict the correlation matrix (Fig. 2(c, d)). Hence, the supervised learning method takes the inputs of the time series of a few nodes as a window ($\Delta \mathbf{T}$) and predicts the correlation matrix ($\tilde{\mathbf{R}}$). The entire correlation matrix is constructed using the symmetry of the matrix with diagonal elements equated to 1 since they are self-correlated. Further, to evaluate the performance during test time, we compare the predicted correlation matrices ($\tilde{\mathbf{R}}_q^k$) from the ML algorithm with the true correlation matrix (\mathbf{R}^k) using Mean Square Error (MSE) measure. Figure 3 shows the MSE between true (\mathbf{R}^k) and predicted ($\tilde{\mathbf{R}}_q^k$) correlation matrices associated to the test data sets. The observations show that prediction accuracy reaches saturation after increasing the number of nodes beyond a certain point. The saturation in accuracy shows that only a limited time series subset is enough to make

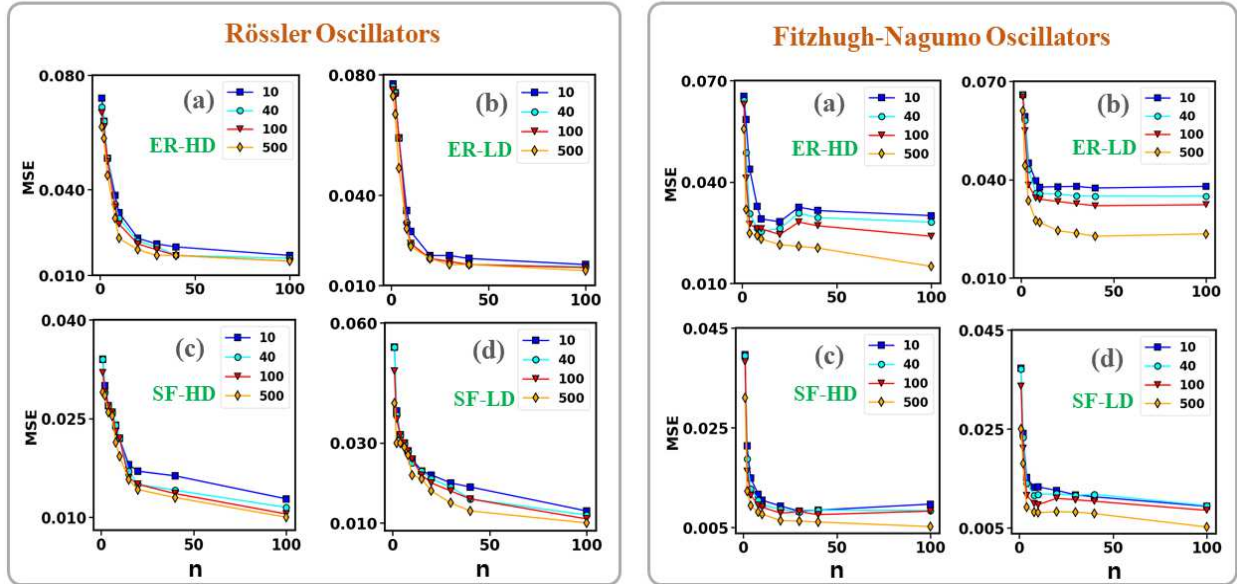


Figure 3: Average Mean Square Error (MSE) between true (\mathbf{R}) and predicted ($\tilde{\mathbf{R}}$) correlation matrices associated with the test data sets for the varying number of nodes (n) and window size. (a, c) the number of higher degree nodes (ER-HD, SF-HD) vs. MSE for ER and SF networks on both the oscillators with varying window size and (b, d) number of lower degree nodes (ER-LD, SF-LD) vs. MSE for ER and SF networks on both the oscillators with varying window size. The plots show saturation in MSE with an increase in n , asserting that only limited nodes are required for predicting the entire correlation matrix for both models. For the oscillators, we choose $\lambda_R = 0.015$, $\lambda_F = 0.32$ for ER network realizations and for the SF network realizations, we consider $\lambda_R = 0.009$, $\lambda_F = 0.28$ and windows sizes $w = \{10, 40, 100, 500\}$.

good correlation matrix predictions. The supervised algorithm predicts the correlation matrices using both higher and lower degree nodes of the network. The prediction accuracy for both cases is observed to be the same (Fig. 3). Thus, the degree of nodes used does not impact the prediction of the correlation matrices. It might be a reason that higher and lower degree nodes are similar due to the small-world effect. As the minimum degree of the networks is greater than 0 and the network is connected, a path exists between a pair of nodes. That is, if we wait for a sufficient time, the information of the entire network can be delivered to the node of the minimum degree. We removed the transient region from the time series; as a result, it is thought that correlated information of the entire network is accumulated in both high and low-degree nodes. For the robustness of our prediction, we vary n and w and create different training and testing data sets, and one can observe that results are the same. Furthermore, we use an unsupervised learning algorithm to show deeper insights into our prediction.

3.3. Unsupervised learning method to understand correlation matrix prediction

Here, we use the UMAP to understand the similarities between predicted ($\tilde{\mathbf{R}}$) and true correlation (\mathbf{R}) matrices by considering whole matrices as points in high dimensional space and embedding them in 2D space. The input to the UMAP is the upper triangular part of all flattened correlation matrices (predicted and true) corresponding to the test data sets. For instance, consider test set contains 75 times-series data sets ($\{\mathbf{T}^1, \mathbf{T}^2, \dots, \mathbf{T}^{75}\}$) and corresponding true correlations matrices ($\{\mathbf{R}^1, \mathbf{R}^2, \dots, \mathbf{R}^{75}\}$) obtain from different ER network realizations on Rössler oscillators. Hence,

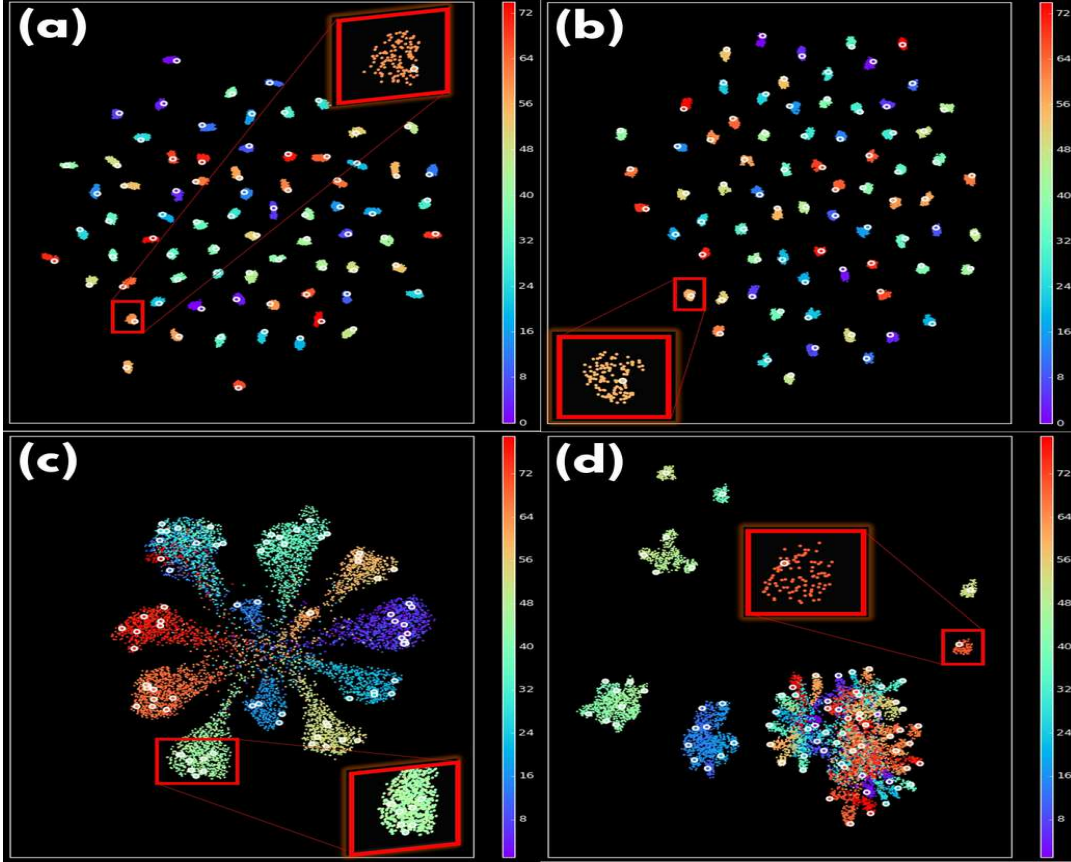


Figure 4: UMAP is generated from the test data sets' predicted and true correlation matrices. The labeled color indicates different test data sets ($\{\mathbf{T}^1, \mathbf{T}^2, \dots, \mathbf{T}^{75}\}$) while white circles represent true correlation matrices ($\{\mathbf{R}^1, \mathbf{R}^2, \dots, \mathbf{R}^{75}\}$). The color dots indicate predicted correlation matrices obtained from different time windows. UMAP for test data sets generated from (a, b) Rössler oscillator on 75 different realizations for ER and SF networks having $\lambda_R = 0.015$. (c, d) FHN oscillator on 75 different realizations for ER and SF networks having $\lambda_F = 0.32$. We consider $n = 40$, $w = 100$ thus $\Delta\mathbf{T} \in \mathbb{R}^{40 \times 100}$.

each \mathbf{T}^k creates $\lceil (5000 - 100)/40 \rceil + 1 = 124$ windows where $w = 100$ and $skip = 40$. Therefore, the total number of predicted correlation matrices from 75 test data sets equals $124 * 75 = 9300$. For the UMAP algorithm, we take the upper triangular part of a correlation matrix and form a high-dimensional vector. The UMAP algorithm takes a high dimensional input vector ($\mathbb{R}^{\frac{N^2-N}{2}}$) and projects it to a point in the lower dimensional plane (\mathbb{R}^2). The process is repeated for all the predicted and true correlation matrices associated with the test data sets.

From Fig. 4(a), one can observe that 75 different clusters correspond to 75 different test time series data sets, each having different colors. Further, in 2D space, true correlation matrices are marked with white colored circles along with the cluster color and predicted correlation matrices form a cloud around the true correlation matrix. Importantly, the predicted and true correlation matrices are close in the 2D space. The predicted correlation matrices for a specific \mathbf{T}^k are distributed only near the corresponding true correlation matrix, inferring that the predictions made are meaningful. The SF network realizations on Rössler oscillator also shows similar behavior as the ER random network realizations (Fig. 4 (a) and (b)).

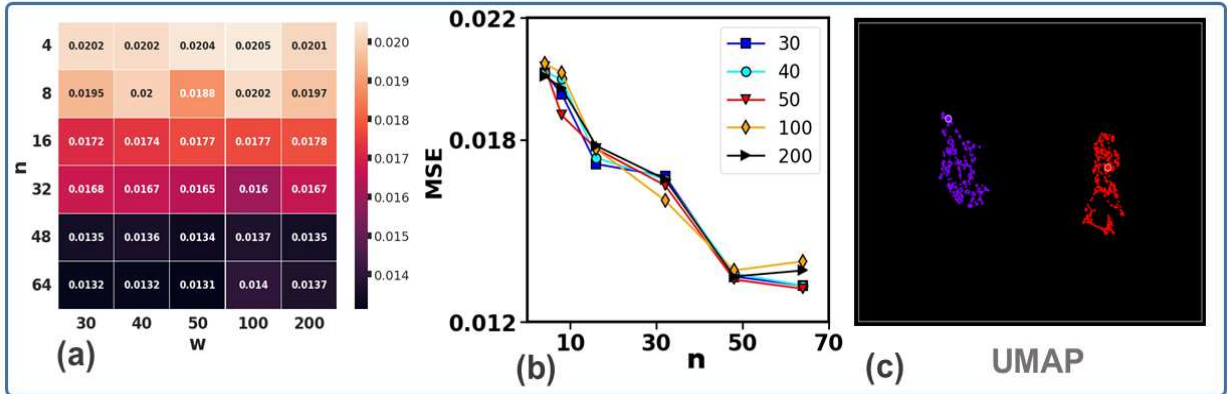


Figure 5: Average Mean Square Error (MSE) between true (\mathbf{R}) and predicted ($\tilde{\mathbf{R}}$) correlation matrices for EEG test data sets. (a) performance array contains MSE of test data sets for varying window size (w) and the number of channels (n) and (b) n vs. MSE with varying window size. The plots show decreasing MSE with an increase in n , asserting that only a limited channel’s EEG time series data are required to predict the entire correlation matrix for EEG data sets. (c) UMAP is generated from the EEG test data sets’ \mathbf{R} and $\tilde{\mathbf{R}}$. Among the EEG data of 65 subjects, two subjects were used as the test data set. The labeled color indicates two different subjects while white circles represent true correlation matrices \mathbf{R} . The color dots embedded points from $\tilde{\mathbf{R}}$ s corresponding to different windows. $\tilde{\mathbf{R}}$ s were generated from $\Delta\mathbf{T} \in \mathbb{R}^{n \times w}$ ($n = 48, w = 50$).

Moreover, one can notice that clusters from 75 different true correlation matrices overlap significantly for the FHN oscillators on the ER and the SF network realizations. However, we can still observe that the predicted correlation matrices are located near the true correlation matrices. The fact that true correlation matrices constitute a cluster means that they share similar characteristics, and the correlation matrices predicted from the model also have these features. Therefore, we can assert that the model makes meaningful predictions (Fig. 4 (c) and (d)).

3.4. Experiment on EEG Data

To validate our model, we use the brain-computer interface data set in our study [26]. The database comprises 64-channel Electroencephalogram (EEG) data of 70 subjects performing a 40-target cued-spelling task. The EEG data are stored as a 4-way tensor, with a dimension of channel \times time point \times block \times condition. Our experiment considers time point vs. channel data for 65 subjects of the first block and condition one. Hence, we have 65 different time series data sets ($\{\mathbf{T}^1, \mathbf{T}^2, \dots, \mathbf{T}^{65}\}$) each of having $N = 64$ time series and length, $L = 750$. From the time series data sets, we create the corresponding true correlation matrices and denoted as ($\{\mathbf{R}^1, \mathbf{R}^2, \dots, \mathbf{R}^{65}\}$).

Among the 65 EEG data sets, we use 63 as training data and 2 data sets used as test data. The training and test sets division are the same as predicting unknown realization in the Rössler and FHN experiments. Further, we create $n \times w$ size windows for the training and test data sets. For instance, for any $\mathbf{T}^k \in \mathbb{R}^{N \times L}$ we have $f = \lceil (L - w) / skip \rceil + 1 = 351$ windows ($\Delta\mathbf{T}_q^k \in \mathbb{R}^{n \times w}$, $1 \leq k \leq 65, 1 \leq q \leq 351$) where $n = 48, w = 50$ and $skip = 2$. Hence, the number of windows for training data sets is $351 * 63 = 22113$ and $351 * 2 = 702$ for the test data sets. We train the model in the training phase by using 22113 windows and 65 true correlation matrices. During the test phase, we use a window in test data sets to predict the correlation matrix ($\tilde{\mathbf{R}}$). We vary n and w to create other training and test data sets and perform the experiment. As shown in Fig. 5 (a) and (b), the MSE decreases as n increases. But for w , it does not affect the performance much until

$w = 200$. The MSE error converges around $n = 48$. If we look at the UMAP for $\tilde{\mathbf{R}}$ and \mathbf{R} , we can see that $\tilde{\mathbf{R}}$ is distributed near the true \mathbf{R} (Fig. 5(c)). In other words, it can be seen that the ML model predicts $\tilde{\mathbf{R}}$, reflecting each subject's unique characteristics. If not, there would be a large overlap in the distribution of \mathbf{R} . Although $\tilde{\mathbf{R}}$ is distributed near the \mathbf{R} , distinct from another \mathbf{R} , it is distributed over a very wide area. It suggests that the model predicts the coarse correlation but does not reflect the detailed information due to a lack of training data size and noise in the EEG data set. With the experimental results obtained from the model and EEG data sets, we expect that the framework can be applied to other real-world data sets as long as enough data sets exist.

4. Conclusion

We have developed an ML framework that predicts the correlation matrix of the entire system from limited time series data available for a subset of nodes. The motivation behind this framework is two folds. The growing interest in exploiting machine learning techniques in predicting time series of networks has led to various outcomes. However, the problem of using only the limited time series data from a few nodes remained challenging. Our framework provides a way to address and resolve this problem.

From the perspective of the progress of the methodology, we present a framework that is a combined effort of supervised and unsupervised learning integrated with appropriate training and testing data sets. The study is focused on making good predictions of the correlation matrices using the limited time series data of a few available nodes. The framework's application is undemanding, given that the data should suffice the condition of being generated from the respective oscillators to be in a semi-synchronous region, which is taken care of by choosing the appropriate coupling strength.

Supervised learning has been applied to make predictions. Its accuracy has been identified by the Mean Square Error, which is the difference between the true and the predicted correlation matrix. The threshold of the number of nodes required and the length of the limited time series to make good predictions have also been discussed. Unsupervised learning (UMAP) brought more insights into the prediction results by visualizing the results. Finally, we use real-world EEG data sets to validate our model. Our work may have opened up a new window into an area of machine learning in complex networks where predictions can be made possible using only a finite time series length and a finite number of nodes of the network and may be relevant to some real-world applications.

Acknowledgment

NE and PL are thankful to Chittaranjan Hens (IIIT Hyderabad) for the useful discussion on the FHN model. PP is indebted to Kritiprassna Das (IIT Indore) for a detailed discussion on the EEG datasets. SJ acknowledges DST grant SPF/2021/000136.

References

- [1] R. Xiao, L. W. Kong, Z. K. Sun, Y. C. Lai, Predicting amplitude death with machine learning, Phys. Rev. E 104 (2021) 014205.
- [2] H. Fan, L. W. Kong, Y. C. Lai, X. Wang, Anticipating synchronization with machine learning, Phys. Rev. Research 3 (2021) 023237.

- [3] Q. Ni, M. Tang, Y. Liu, Y.C. Lai, Machine learning dynamical phase transitions in complex networks, *Phys. Rev. E* 100 (2019) 052312.
- [4] S. Ghosh, A. Senapati, A. Mishra, J. Chattopadhyay, S. K. Dana, C. Hens, D. Ghosh, Reservoir computing on epidemic spreading: A case study on covid-19 cases, *Physical Review E* 104 (1) (2021) 014308.
- [5] J. Pathak, B. Hunt, M. Girvan, Z. Lu, E. Ott, Model-free prediction of large spatiotemporally chaotic systems from data: A reservoir computing approach, *Phys. Rev. Lett.* 120 (2018) 024102.
- [6] H. Fan, J. Jiang, C. Zhang, X. Wang, Y.C. Lai, Long-term prediction of chaotic systems with machine learning, *Phys. Rev. Research* 2 (2020) 012080.
- [7] K. Schindler, H. Leung, C. E. Elger, K. Lehnertz, Assessing seizure dynamics by analysing the correlation structure of multichannel intracranial eeg, *Brain* 130 (1) (2007) 65-77.
- [8] V. Plerou, P. Gopikrishnan, B. Rosenow, L. A. Nunes Amaral, H. E. Stanley, Universal and nonuniversal properties of cross correlations in financial time series, *Phys. Rev. Lett.* 83 (1999) 1471-1474.
- [9] S. Bialonski, M. T. Horstmann, K. Lehnertz, From brain to earth and climate systems: Small-world interaction networks or not?, *Chaos: An Interdisciplinary Journal of Nonlinear Science* 20 (1) (2010) 013134.
- [10] V. M. Eguiluz, D. R. Chialvo, G. A. Cecchi, M. Baliki, A. V. Apkarian, Scale-free brain functional networks, *Physical review letters* 94 (1) (2005) 018102.
- [11] J. Schiefer, A. Niederbuhl, V. Pernice, C. Lennartz, J. Hennig, P. LeVan, S. Rotter, From correlation to causation: Estimating effective connectivity from zero-lag covariances of brain signals, *PLoS computational biology* 14 (3) (2018) e1006056.
- [12] J. Friedman, T. Hastie, R. Tibshirani, Sparse inverse covariance estimation with the graphical lasso, *Biostatistics* 9 (3) (2008) 432-441.
- [13] A. L. Barabasi, R. Albert, Emergence of scaling in random networks, *science* 286 (5439) (1999) 509-512.
- [14] A. Blum, J. Hopcroft, R. Kannan, *Foundations of data science*, Cambridge University Press, 2020.
- [15] M. G. Rosenblum, A. S. Pikovsky, J. Kurths, Phase synchronization of chaotic oscillators, *Physical review letters* 76 (11) (1996) 1804.
- [16] A. L. Hodgkin, A. F. Huxley, A quantitative description of membrane current and its application to conduction and excitation in nerve, *The Journal of physiology* 117 (4) (1952) 500.
- [17] R.Q. Su, Y.C. Lai, X. Wang, Identifying chaotic fitzhugh-nagumo neurons using compressive sensing, *Entropy* 16 (7) (2014) 3889-3902.
- [18] I. Goodfellow, Y. Bengio, A. Courville, *Deep learning*, MIT press, 2016.

- [19] G. Klambauer, T. Unterthiner, A. Mayr, S. Hochreiter, Self-normalizing neural networks, in: Proceedings of the 31st international conference on neural information processing systems, 2017, pp. 972-981.
- [20] D. P. Kingma, J. Ba, Adam: A method for stochastic optimization, arXiv preprint arXiv:1412.6980 (2014).
- [21] T. Fujiwara, N. Sakamoto, J. Nonaka, K. Yamamoto, K.L. Ma, et al., A visual analytics framework for reviewing multivariate time-series data with dimensionality reduction, IEEE transactions on visualization and computer graphics 27 (2) (2020) 1601-1611.
- [22] D. Freedman, R. Pisani, R. Purves, Statistics (international student edition), Pisani, R. Purves, 4th edn. WW Norton and Company, New York (2007).
- [23] O. I. Moskalenko, A. A. Koronovskii, A. E. Hramov, S. Boccaletti, Generalized synchronization in mutually coupled oscillators and complex networks, Physical Review E 86 (3) (2012) 036216.
- [24] G. Tirabassi, R. Sevilla-Escoboza, J. M. Buldu, C. Masoller, Inferring the connectivity of coupled oscillators from time-series statistical similarity analysis, Scientific reports 5 (1) (2015) 1-14.
- [25] C. Wissler, The spearman correlation formula, Science 22 (558) (1905) 309-311.
- [26] B. Liu, X. Huang, Y. Wang, X. Chen, X. Gao, Beta: A large benchmark database towards svepbci application, Frontiers in neuroscience 14 (2020) 627.